Annales Geophysicae (2004) 22: 2171–2179
SRef-ID: 1432-0576/ag/2004-22-2171


Annales Geophysicae

# Resonant three-wave interaction in the presence of suprathermal electron fluxes

**C. Krafft**[1] **and A. Volokitin**[2]

[1]Laboratoire de Physique des Gaz et des Plasmas, Université Paris Sud, 91405 Orsay Cedex, France
[2]Institute of Terrestrial Magnetism, Ionosphere and Radiowave Propagation, Academy of Sciences, Troitsk, Moscow Region, 142190, Russia

Received: 7 October 2003 – Revised: 2 February 2004 – Accepted: 18 February 2004 – Published: 14 June 2004

**Abstract.** A theoretical and numerical model is presented which describes the nonlinear interaction of lower hybrid waves with a non-equilibrium electron distribution function in a magnetized plasma. The paper presents some relevant examples of numerical simulations which show the nonlinear evolution of a set of three waves interacting at various resonance velocities with a flux of electrons presenting some anisotropy in the parallel velocity distribution (suprathermal tail); in particular, the case when the interactions between the waves are neglected (for sufficiently small waves' amplitudes) is compared to the case when the three waves follow a resonant decay process. A competition between excitation (due to the fan instability with tail electrons or to the bump-in-tail instability at the Landau resonances) and damping processes (involving bulk electrons at the Landau resonances) takes place for each wave, depending on the strength of the wave-wave coupling, on the linear growth rates of the waves and on the modifications of the particles' distribution resulting from the linear and nonlinear wave-particle interactions. It is shown that the energy carried by the suprathermal electron tail is more effectively transfered to lower energy electrons in the presence of wave-wave interactions.

**Key words.** Space plasma physics (wave-particle interactions, waves and instabilities, wave-wave interactions)

## 1 Introduction

Lower hybrid and whistler waves have been currently observed in space plasmas as the terrestrial magnetosphere or the solar wind. Moreover, several in-situ measurements have evidenced their presence simultaneously with suprathermal fluxes or beams of electrons; for example, they are believed to play a role in solar type III radio bursts (Lin et al., 1981, 1986, 1998; Kellogg et al., 1992a, 1992b; Reiner et al., 1992; Stone et al., 1995; Thejappa et al., 1995; Ergun et al., 1998; Thejappa and MacDowall, 1998; Moullard et al., 1998, 2001) and in wave-particle processes occurring in the auroral ionosphere (Ergun et al., 1993; Muschietti et al., 1997) or in the terrestrial electron foreshock, for example (Hoppe et al., 1982; Zhang et al., 1999). Many questions deserve up to now to be raised concerning the generation mechanisms of the observed waves, the processes that govern the high-energy fluxes' evolution and the role of nonlinear wave-particle and wave-wave interactions. The study presented here, which models the interaction of a set of waves with a non-equilibrium electron velocity distribution in a magnetized plasma, contributes to clarify what mechanisms should to be taken into account or should be neglected for a correct description of physical situations as those cited above.

*Correspondence to:* C. Krafft
(catherine.krafft@pgp.u-psud.fr)

In order to study the nonlinear interaction of such waves with electron beams and fluxes, two approaches have been mainly considered up to now in the literature (e.g. O'Neil et al., 1971; Shapiro and Shevchenko, 1968, 1971; Matsiborko et al., 1972, 1973; Kovalenko, 1983; Pivovarov et al., 1995; Volokitin and Krafft, 2000, 2001a, 2001b, 2004; Krafft et al., 2000; Krafft and Volokitin, 2002, 2003a): first, the study of the instability and the saturation processes of a single monochromatic wave (which can be used for the modeling of some experimental situations in laboratory), and second, the evolution of a wide spectrum of waves at the stage when the turbulence is well developed. However, the intermediate case, when only a few wave modes are governing the nonlinear processes through their mutual interaction and their interaction with the particles, has also to be considered for the adequate modeling of some space plasma phenomena.

We present in this paper a theoretical and numerical model which describes the nonlinear interaction of lower hybrid waves with suprathermal fluxes of electrons, and, more generally, which allows one to consider various physical situations involving the interaction of waves with a non-equilibrium electron distribution function. This Hamiltonian self-consistent model is based on a semi-analytical approach and provides an efficient and original tool to study the various features of the wave-particle and wave-wave interactions.

Indeed, the analytical treatment performed to obtain the potential evolution as a simple linear differential equation leads eventually to a crucial decrease in the computing time and to evidence clear and interpretable physical results. Moreover, this approach allows one to present the wave-particle system in a Hamiltonian form and thus to use symplectic methods for the fields' evolution and the particle's motion numerical calculations.

Lower hybrid waves can be driven unstable by the presence of some anisotropy in the electron velocity distribution along the ambient magnetic field, as it was first discussed in the frame of thermonuclear fusion by Kadomtsev and Pogutse (1967): this so-called "fan instability", where energetic electrons interact with the wave at the anomalous cyclotron resonance, does not require any positive slope in the suprathermal electron tail (Shapiro and Shevchenko, 1968; Haber et al., 1978). Its threshold is overcome if the number of electrons giving energy to the wave interacting at the anomalous cyclotron resonance exceeds the number of electrons taking energy from the wave at the Landau and the normal cyclotron resonances (Mikhailovskii, 1974; Omelchenko et al., 1994; Krafft and Volokitin, 2003b). This instability is worth being studied in the frame of our model, when one given wave is simultaneously involved in several resonant interaction processes; for example, a wave excited by the fan instability through its interaction with some tail electrons at the anomalous cyclotron resonance can be simultaneously damped at the Landau resonance (interaction with the thermal bulk electrons) and at the normal cyclotron resonance (interaction with a very small amount of electrons of negative parallel velocity). This competition between excitation and damping processes, which takes place for each wave, can lead in the nonlinear stage to new physical effects when considering a set of several waves: for example, if a wave is stable in the linear stage, it can become unstable during the nonlinear evolution as a result of the modification of the particles' velocity distribution functions through the action of the other waves. Moreover, the wave-wave coupling can enhance the interaction between the waves and the particles.

This paper presents some relevant examples of numerical simulations showing the nonlinear evolution of a set of three waves interacting at various resonances (Landau, anomalous and normal cyclotron) with a flux of electrons which presents some anisotropy in the parallel velocity distribution; in particular, the case when the interactions between the waves are neglected (for sufficiently small waves' amplitudes) is compared to the case when the three waves follow a resonant decay process.

## 2 Nonlinear model for lower hybrid wave-particle interaction

The equation describing the evolution of the potential $\varphi(\boldsymbol{r}_\perp, z, t)$ of an electrostatic lower hybrid wave of frequency $\omega$ (in the range $\omega_{lh}=\omega_{pi}\omega_c/\left(\omega_c^2+\omega_p^2\right)^{1/2} \ll \omega \leq \omega_c$, where $\omega_{lh}$, $\omega_{pi}$, $\omega_c$ and $\omega_p$ are the lower hybrid, the ion plasma, the electron cyclotron and the electron plasma frequencies, respectively) under the influence of a beam or a flux of suprathermal electrons of density $n_h$ in a background magnetized plasma (the ambient magnetic field is uniform and directed along the z axis, $\boldsymbol{B}_0=B_0\boldsymbol{z}$) is given by (Volokitin and Krafft, 2001a, Krafft and Volokitin, 2002)

$$\frac{\partial^2}{\partial t^2}\left(1+\frac{\omega_p^2}{\omega_c^2}\right)\boldsymbol{\nabla}^2\varphi+\omega_p^2\frac{\partial^2\varphi}{\partial z^2}=\frac{\partial^2}{\partial t^2}4\pi e n_h, \tag{1}$$

with $n_h \equiv n_b \int f_h\left(\boldsymbol{v},\boldsymbol{r},t\right) d^3\boldsymbol{v}$; $f_h\left(\boldsymbol{v},\boldsymbol{r},t\right)$ is the distribution function of the suprathermal electron population; $\boldsymbol{r}\left(\boldsymbol{r}_\perp, z\right)$ is the coordinate and $\boldsymbol{v}\left(\boldsymbol{v}_\perp, v_z\right)$ is the velocity; $-e<0$ is the electron charge. Equation (1), which can be derived from the Poisson, the fluid and the continuity equations, allows one to obtain the dispersion relation of the electrostatic lower hybrid waves ($\frac{\omega_p^2}{c^2k^2}\ll 1$), that is

$$\frac{\omega^2}{\omega_c^2}\simeq\frac{k_z^2}{k^2}\frac{\omega_p^2}{\omega_c^2+\omega_p^2},$$

where $\boldsymbol{k}(k_z,k_\perp)$ is the wave vector. The ions form a motionless neutralizing background and their dynamics is not essential in the range of frequencies considered. Assuming that the wave-particle interactions are relatively weak and that the lower hybrid wave potential $\varphi$ can be presented as the sum of waves with potential amplitudes $\varphi_{\boldsymbol{k}}$ slowly varying along $\boldsymbol{z}$, that is $\varphi\left(\boldsymbol{r}_\perp,z,t\right)=\mathrm{Re}\sum_{\boldsymbol{k}}\varphi_{\boldsymbol{k}}\left(z,t\right)\exp\left(ik_zz+i\boldsymbol{k}_\perp\cdot\boldsymbol{r}_\perp-i\omega_{\boldsymbol{k}}t\right)$ (it is assumed that the plasma and the electron flux are homogeneous along the direction perpendicular to the ambient magnetic field), we obtain in Fourier presentation

$$\frac{\partial\varphi_{\boldsymbol{k}}}{\partial t}+v_{gz}\frac{\partial\varphi_{\boldsymbol{k}}}{\partial z}=\frac{i\omega_{\boldsymbol{k}}}{\boldsymbol{k}^2}\frac{4\pi e n_b\omega_c^2}{\omega_c^2+\omega_p^2} \tag{2}$$

$$\left\langle\int\frac{d^2rdz}{L_zL_\perp^2}\int d^3\boldsymbol{v}\exp\left(-ik_zz-i\boldsymbol{k}_\perp\cdot\boldsymbol{r}_\perp+i\omega_{\boldsymbol{k}}t\right)f_h\left(\boldsymbol{v},\boldsymbol{r},t\right)\right\rangle,$$

which gives, for a plasma and a flux homogeneous along $z$

$$\frac{\partial\varphi_{\boldsymbol{k}}}{\partial t}\simeq\frac{i\omega_{\boldsymbol{k}}}{\boldsymbol{k}^2}\frac{4\pi e n_b\omega_c^2}{\omega_c^2+\omega_p^2} \tag{3}$$

$$\left\langle\int\frac{d^2rdz}{L_zL_\perp^2}\int d^3\boldsymbol{v}\exp\left(-ik_zz-i\boldsymbol{k}_\perp\cdot\boldsymbol{r}_\perp+i\omega_{\boldsymbol{k}}t\right)f_h\left(\boldsymbol{v},\boldsymbol{r},t\right)\right\rangle,$$

where $v_{gz}=\frac{\omega_p^2\omega_c^2k_z}{\boldsymbol{k}^2\omega_{\boldsymbol{k}}\left(\omega_c^2+\omega_p^2\right)}=\frac{\partial\omega_{\boldsymbol{k}}}{\partial k_z}$ is the parallel group velocity; $L_z$ and $L_\perp$ are the spatial periods in the parallel and the perpendicular directions, respectively. The nonlinear terms corresponding to wave-wave coupling (neglected in Eq. (2)) will be examined in detail below. The averaging $\langle\rangle\leftrightarrow\int\frac{dt}{T}$ is performed on a wave period $T=2\pi/\omega$. Moreover, using the conservation of the phase space volume along the particles' trajectories, one can express Eq. (2) as a function of the total number of macro-particles $N$ inside the box of volume $L_z L_\perp^2$, where $L_z = 2\pi/k_{z\,\min}$ and $L_\perp = 2\pi/k_{\perp\,\min}$ ($k_{z\,\min}$ and $k_{\perp\,\min}$) are the minimum values of the parallel and the perpendicular wave numbers, respectively), with the help of

$$\int \frac{d^2 r dz}{L_z L_\perp^2} \int d^3 \boldsymbol{v} f_h(\boldsymbol{v}, \boldsymbol{r}, t) \to \frac{1}{N} \sum_{p=1}^{N}, \quad N = n_b L_z L_\perp^2, \quad (4)$$

Note that, as shown by our numerical simulations (see below and Volokitin and Krafft, 2004), the operation of time averaging $\langle\rangle$ can be omitted without any violation of the model validity. Finally, one obtains the nonlinear evolution of the potential amplitude (2) in the form

$$\frac{\partial}{\partial t}\left(\frac{e\varphi_{\boldsymbol{k}}}{m_e v_*^2}\right)$$

$$\simeq \frac{i\omega_{\boldsymbol{k}}\omega_p^2}{\omega_c^2+\omega_p^2}\frac{\omega_c^2}{\boldsymbol{k}^2 v_*^2}\frac{n_b}{n_0}\frac{1}{N}\sum_{p=1}^{N}\exp\left(-i\eta_p\right), \quad (5)$$

where $\eta_p = k_z z_p + \boldsymbol{k}_\perp \cdot \boldsymbol{r}_{\perp p} - \omega_{\boldsymbol{k}} t$ is the phase of the particle $p$ located at the position $\boldsymbol{r}_p(\boldsymbol{r}_{\perp p}, z_p, t)$; $v_*$ is the normalization velocity and $m_e$ is the electron mass; $n_0$ is the background plasma density.

The motion of the electrons in the wave fields is described by

$$\frac{d\boldsymbol{r}}{dt} = \boldsymbol{v}, \quad \frac{d\boldsymbol{v}}{dt} + \boldsymbol{v} \times \boldsymbol{\omega_c} = \frac{e}{m_e}\nabla\varphi$$

$$= \frac{ie}{m_e}\mathrm{Re}\sum_{\boldsymbol{k}} \boldsymbol{k}\varphi_{\boldsymbol{k}}(t)\exp\left(ik_z z + i\boldsymbol{k}_\perp \cdot \boldsymbol{r}_\perp - i\omega_{\boldsymbol{k}} t\right), \quad (6)$$

where $\boldsymbol{\omega}_c = \frac{e\boldsymbol{B}_0}{m_e c} = \omega_c \frac{\boldsymbol{B}_0}{B_0}$ (all nonlinearities are kept in the motion Eq. (6)). Note that the Eqs. (5)–(6) have a Hamiltonian structure. Indeed, introducing the generalized impulse of the particle $p$ as $\boldsymbol{p}_p = m_e \boldsymbol{v}_p - eB_0(\boldsymbol{z} \times \boldsymbol{r}_p)/c = m_e(\boldsymbol{v}_p - \boldsymbol{\omega}_c \times \boldsymbol{r}_p)$, Eq. (6) can be expressed as follows

$$\frac{\partial \boldsymbol{p}_p}{\partial t} = -\frac{\partial H_p}{\partial \boldsymbol{r}_p} = e\mathrm{Re}\sum_{\boldsymbol{k}} i\boldsymbol{k}\varphi_{\boldsymbol{k}}\exp\left(i\boldsymbol{k}\cdot\boldsymbol{r}_p - i\omega_{\boldsymbol{k}} t\right), \quad (7)$$

$$\frac{\partial \boldsymbol{r}_p}{\partial t} = \frac{\partial H_p}{\partial \boldsymbol{p}_p} = \boldsymbol{v}_p, \quad (8)$$

with

$$H_p = \sum_p$$

$$\left[\frac{\left(\boldsymbol{p}_p + e\boldsymbol{A}/c\right)^2}{2m_e} - \mathrm{Re}\sum_{\boldsymbol{k}} e\varphi_{\boldsymbol{k}}\exp\left(i\boldsymbol{k}\cdot\boldsymbol{r}_p - i\omega_{\boldsymbol{k}} t\right)\right], \quad (9)$$

where $\boldsymbol{A}$ is the vector potential (here $\nabla \times \boldsymbol{A} = \boldsymbol{B}_0$). Then, introducing the normal wave amplitudes as

$$C_{\boldsymbol{k}}(t) = \sqrt{L_z L_\perp^2 \frac{\omega_c^2+\omega_p^2}{\omega_{\boldsymbol{k}}\omega_c^2}\frac{\boldsymbol{k}^2}{8\pi}}\varphi_{\boldsymbol{k}}(t)\exp\left(-i\omega_{\boldsymbol{k}} t\right), \quad (10)$$

and noting that

$$-\frac{e}{2}\sum_p \exp\left(i\omega_{\boldsymbol{k}} t - i\boldsymbol{k}\cdot\boldsymbol{r}_p\right) = \frac{\partial H_p}{\partial \varphi_{\boldsymbol{k}}^*}, \quad (11)$$

the Eq. (5) can be presented as

$$\frac{\partial C_{\boldsymbol{k}}}{\partial t} = -i\omega_{\boldsymbol{k}} C_{\boldsymbol{k}} + \frac{ie}{2}\frac{\exp\left(-i\omega_{\boldsymbol{k}} t\right)}{\sqrt{L_\perp^2 L_z \frac{\omega_c^2+\omega_p^2}{\omega_{\boldsymbol{k}}\omega_c^2}\frac{\boldsymbol{k}^2}{8\pi}}}$$

$$\sum_p \exp\left(i\omega_{\boldsymbol{k}} t - i\boldsymbol{k}\cdot\boldsymbol{r}_p\right) = -i\frac{\partial H}{\partial C_{\boldsymbol{k}}^*}, \quad (12)$$

with

$$H = H_p + H_0,$$

$$H_0 = \sum_{\boldsymbol{k}} \omega_{\boldsymbol{k}} |C_{\boldsymbol{k}}|^2 = L_\perp^2 L_z \sum_{\boldsymbol{k}} \frac{\omega_c^2+\omega_p^2}{\omega_c^2}\frac{|\boldsymbol{k}\varphi_{\boldsymbol{k}}|^2}{8\pi}, \quad (13)$$

where $H_0$ is the energy of the free waves in the volume $L_\perp^2 L_z$.

## 3 Wave-wave interaction terms

The wave-wave interactions can be included in the presented model by adding to the Hamiltonian (13) some term describing the coupling between the waves; for a three-wave resonant process with matching conditions $\boldsymbol{k}(\boldsymbol{k}_\perp, k_z) = \boldsymbol{k}_1(\boldsymbol{k}_{\perp 1}, k_{z1}) + \boldsymbol{k}_2(\boldsymbol{k}_{\perp 2}, k_{z2})$ and $\omega_{\boldsymbol{k}} = \omega_{\boldsymbol{k}_1} + \omega_{\boldsymbol{k}_2}$, it can be written in the following form

$$H_{int} = \frac{1}{\sqrt{L_\perp^2 L_z}} \sum_{\boldsymbol{k}=\boldsymbol{k}_1+\boldsymbol{k}_2} V_{\boldsymbol{k}\boldsymbol{k}_1\boldsymbol{k}_2} C_{\boldsymbol{k}}^* C_{\boldsymbol{k}_1} C_{\boldsymbol{k}_2} + c.c., \quad (14)$$

where the wave-wave interaction matrix element $V_{\boldsymbol{k}\boldsymbol{k}_1\boldsymbol{k}_2}$ satisfies to some rules of symmetry. For the case of lower hybrid waves, the calculations give

$$V_{\boldsymbol{k}\boldsymbol{k}_1\boldsymbol{k}_2} = -\frac{\left(8\pi\omega_{\boldsymbol{k}_1}\omega_{\boldsymbol{k}_2}\right)^{1/2}\omega_p^2\omega_c^3}{kk_1k_2\omega_{\boldsymbol{k}}^{1/2}\left(\omega_c^2+\omega_p^2\right)^{3/2}}\frac{e}{8m_e}$$

$$\left\{\frac{k_z^2 k_{z1} k_{z2}}{\omega_{\boldsymbol{k}}\omega_{\boldsymbol{k}_1}\omega_{\boldsymbol{k}_2}} + \frac{k_1^2 k_z k_{z2}}{\omega_p^2\omega_{\boldsymbol{k}_2}} + \frac{k_2^2 k_z k_{z1}}{\omega_p^2\omega_{\boldsymbol{k}_1}} + \frac{k_{z1}k_{z2}\left(\boldsymbol{k}_\perp\cdot\boldsymbol{k}_{\perp 2}\right)}{\omega_c^2\omega_{\boldsymbol{k}_1}}\right.$$

$$+\frac{k_{z1}k_{z2}\left(\boldsymbol{k}_\perp\cdot\boldsymbol{k}_{\perp 1}\right)}{\omega_c^2\omega_{\boldsymbol{k}_2}} + \frac{i}{\omega_c}$$

$$\left.\left[\frac{k_z}{\omega_{\boldsymbol{k}}}\left(\frac{k_{z1}}{\omega_{k1}} - \frac{k_{z2}}{\omega_{k2}}\right) + \left(1+\frac{\omega_p^2}{\omega_c^2}\right)\frac{k_1^2-k_2^2}{\omega_p^2}\right](\boldsymbol{k}_1\times\boldsymbol{k}_2)\cdot\boldsymbol{z}\right\} \quad (15)$$

where $k$, $k_1$ and $k_2$ are the moduli of the wave vectors $\boldsymbol{k}$, $\boldsymbol{k}_1$ and $\boldsymbol{k}_2$. Using the normal amplitudes, the full equations for the waves are given by

$$\frac{\partial C_{\boldsymbol{k}}}{\partial t} = -i\frac{\partial H}{\partial C_{\boldsymbol{k}}^*} = -i\omega_{\boldsymbol{k}} C_{\boldsymbol{k}}$$

$$+\frac{ie}{2}\frac{1}{\sqrt{L_\perp^2 L_z \frac{\omega_c^2+\omega_p^2}{\omega_{\boldsymbol{k}}\omega_c^2}\frac{\boldsymbol{k}^2}{8\pi}}}\sum_{p=1}^{N}\exp\left(-i\boldsymbol{k}\cdot\boldsymbol{r}_p\right)$$

$$-\frac{i}{\sqrt{L_\perp^2 L_z}}\left(\sum_{\boldsymbol{k}=\boldsymbol{k}_1+\boldsymbol{k}_2} V_{\boldsymbol{k}\boldsymbol{k}_1\boldsymbol{k}_2}C_{\boldsymbol{k}_1}C_{\boldsymbol{k}_2}\right), \tag{16}$$

whereas the two other coupled differential equations can be obtained by performing adequate permutations of the wave numbers in Eq. (16), according to the symmetry rules. Returning to the wave potential $\varphi_{\boldsymbol{k}}$ we obtain

$$\frac{\partial}{\partial t}\left(\frac{e\varphi_{\boldsymbol{k}}}{m_e v_*^2}\right)+i\left(\sum_{\boldsymbol{k}=\boldsymbol{k}_1+\boldsymbol{k}_2}\omega_c\Gamma_{\boldsymbol{k}_1\boldsymbol{k}_2}\left(\frac{e\varphi_{\boldsymbol{k}_1}}{m_e v_*^2}\right)\right.$$
$$\left.\left(\frac{e\varphi_{\boldsymbol{k}_2}}{m_e v_*^2}\right)e^{i\left(\omega_{\boldsymbol{k}}-\omega_{\boldsymbol{k}_1}-\omega_{\boldsymbol{k}_2}\right)t}\right)$$
$$=\frac{i\omega_{\boldsymbol{k}}\omega_p^2}{\omega_c^2+\omega_p^2}\frac{\omega_c^2}{\boldsymbol{k}^2 v_*^2}\frac{n_b}{n_0}\frac{1}{N}\sum_{p=1}^{N}\exp\left(-i\eta_p\right), \tag{17}$$

where the coefficients of interaction $\Gamma_{\boldsymbol{k}_1\boldsymbol{k}_2}$ relate to the matrix elements $V_{\boldsymbol{k}\boldsymbol{k}_1\boldsymbol{k}_2}$ according to

$$\Gamma_{\boldsymbol{k}_1\boldsymbol{k}_2}=\frac{m_e v_*^2}{e\omega_c}\frac{k_1k_2}{k}\sqrt{\frac{\omega_{\boldsymbol{k}}}{\omega_{\boldsymbol{k}_1}\omega_{\boldsymbol{k}_2}}}\sqrt{\frac{\omega_c^2+\omega_p^2}{8\pi\omega_c^2}}V_{\boldsymbol{k}\boldsymbol{k}_1\boldsymbol{k}_2}. \tag{18}$$

Due to the Hamiltonian nature of the system, its total energy, which coincides with the total Hamiltonian

$$H=\sum_{p=1}^{N}\left[\frac{m_e\boldsymbol{v}_p^2}{2}-\mathrm{Re}\sum_{\boldsymbol{k}}e\varphi_{\boldsymbol{k}}\exp\left(i\boldsymbol{k}\cdot\boldsymbol{r}_p-i\omega_{\boldsymbol{k}}t\right)\right]$$
$$+L_\perp^2 L_z\left(\frac{\omega_c^2+\omega_p^2}{\omega_c^2}\right)\left[\sum_{\boldsymbol{k}}\frac{|\boldsymbol{k}\varphi_{\boldsymbol{k}}|^2}{8\pi}+\sum_{\boldsymbol{k}=\boldsymbol{k}_1+\boldsymbol{k}_2}\left(\left(\frac{\omega_c^2+\omega_p^2}{\omega_c^2}\right)^{1/2}\right.\right.$$
$$\left.\left.\frac{kk_1k_2V_{\boldsymbol{k}\boldsymbol{k}_1\boldsymbol{k}_2}\varphi_{\boldsymbol{k}}^*\varphi_{\boldsymbol{k}_1}\varphi_{\boldsymbol{k}_2}}{(8\pi)^{3/2}\sqrt{\omega_{\boldsymbol{k}}\omega_{\boldsymbol{k}_1}\omega_{\boldsymbol{k}_2}}}e^{i\left(\omega_{\boldsymbol{k}}-\omega_{\boldsymbol{k}_1}-\omega_{\boldsymbol{k}_2}\right)t}+c.c.\right)\right], \tag{19}$$

and its total impulse

$$P_z=\sum_{p=1}^{N}m_e v_{zp}+L_\perp^2 L_z\left(\frac{\omega_c^2+\omega_p^2}{\omega_c^2}\right)\sum_{\boldsymbol{k}}\frac{k_z}{\omega_{\boldsymbol{k}}}\frac{|\boldsymbol{k}\varphi_{\boldsymbol{k}}|^2}{8\pi} \tag{20}$$

are conserved.

## 4 Numerical simulation results

The first results provided by the numerical simulations based on Eqs. (5)–(6) (without the wave-wave interaction terms) are presented in Volokitin and Krafft (2004), where different instabilities of lower hybrid waves driven by suprathermal electron fluxes in a magnetized plasma have been considered. In this paper we are mainly interested in studying the nonlinear stage of the evolution of three waves interacting with a suprathermal electron flux at the Landau, the normal and/or the anomalous cyclotron resonance velocities (that is, $v_R=(\omega-m\omega_c)/k_z$ for $m$=0, $m$=1 and $m$=−1, respectively). Indeed, we consider a lower hybrid wave $(\boldsymbol{k}, \omega_{\boldsymbol{k}})$ which is excited by the fan instability and decays resonantly in two other lower hybrid waves $(\boldsymbol{k}_1, \omega_{\boldsymbol{k}_1})$ and $(\boldsymbol{k}_2, \omega_{\boldsymbol{k}_2})$, whereas satisfying the matching conditions $\boldsymbol{k}=\boldsymbol{k}_1+\boldsymbol{k}_2$ and $\omega_{\boldsymbol{k}}=\omega_{\boldsymbol{k}_1}+\omega_{\boldsymbol{k}_2}$; each of the three waves can interact with the particles at several resonance velocities simultaneously. The following numerical results are presented in a dimensionless form: the time is normalized by the electron cyclotron period, $\tau=\omega_c t/2\pi$, the particles' velocities are measured in units of some typical velocity $v_*$, all space coordinates are normalized by the corresponding Larmor radius $v_*/\omega_c$ and the normalized wave potentials are $e\varphi_{\boldsymbol{k}}/m_e v_*^2$. As a result, the normalized equation of the potential evolution (17) contains the dimensionless parameter $p=\frac{\omega_p^2}{\omega_c^2+\omega_p^2}\frac{n_b}{n_0}<1$ which describes the electron flux intensity. All normalized variables used below are described by the same notations as the physical ones. Let us note that, because we study the interaction of a wave with electron fluxes in strongly non-equilibrium states, as, for example, with particle distributions of different perpendicular and parallel temperatures, the typical energy of the plasma electrons can differ from the thermal energy; however, in most cases, it is possible to consider that it is close to the characteristic energy of the bulk electrons. The total velocity distribution function is constituted by two populations of electrons: the bulk (or the core) and the tail. In general, for instabilities involving energetic electrons, the thermal bulk electrons are non-resonant and do not participate directly in the wave-particle interaction, even if they influence on the waves through the dielectric tensor; the tail involves the suprathermal electrons which can be in cyclotron resonance with the waves. Thus, in the numerical simulations, in order to point out clearly the wave excitation mechanisms at work, the bulk electrons are generally not represented as macro-particles; however, their interaction with particles can be modeled by taking into account some Landau damping through the introduction of a distribution function in the bulk region. The tail electrons are distributed uniformly in space within a numerical box of size $[L_x, L_y, L_z]=[L_\perp, L_\perp, L_z]$ with periodic boundary conditions; this box contains a finite number of wavelengths of each wave present in the system. The particle velocity distributions can model a very wide set of physically interesting distributions, ranging in the parallel direction up to several tens of thermal velocities. These nonuniform distributions are loaded using classical methods as the method of inversion of cumulative distribution functions. The electrons are distributed in phase space either randomly, or using quiet start methods, in order to decrease the numerical noise; in the latter case, the distributions are sampled using the so-called Hemmersley's sequence. The normalized first order differential equation governing the potential is solved at each time step using a finite-difference numerical scheme; the Newton-Lorentz equations are computed self-consistently owing to the usual leap-frog method. It is worth noting that in all calculations the accuracy of the conservation with the time of

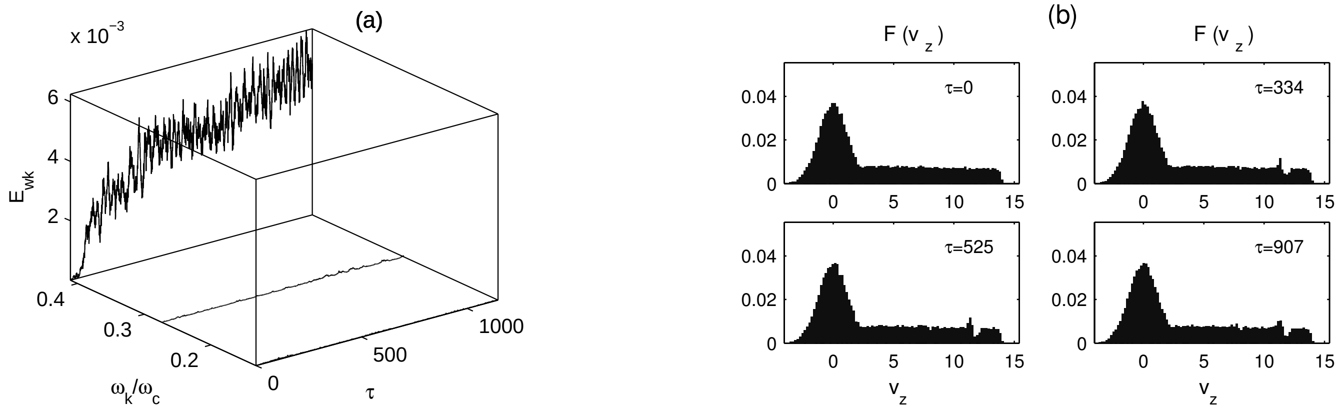


**Fig. 1.** Interaction of three waves with a particle distribution in the presence of a suprathermal tail of electrons extending in the parallel direction $v_z>0$. The waves' frequencies and wave vectors are satisfying the matching conditions: $\boldsymbol{k}=\boldsymbol{k}_1+\boldsymbol{k}_2$ and $\omega_{\boldsymbol{k}}=\omega_{\boldsymbol{k}_1}+\omega_{\boldsymbol{k}_2}$; the coupling between the three waves is neglected. **(a)** Variation as a function of the normalized time $\tau=\omega_c t/2\pi$ of the normalized wave energy density $E_{wk}$ (proportional to $\left|\varphi_{\boldsymbol{k}}^2\right|$) of each of the three waves (each wave is indicated by its normalized frequency $\omega_{\boldsymbol{k}}/\omega_c$): the amplitudes of the second and third waves, $\left(\omega_{\boldsymbol{k}_1},\boldsymbol{k}_1\right)$ and $\left(\omega_{\boldsymbol{k}_2},\boldsymbol{k}_2\right)$, are negligibly small compared to that of the first one; **(b)** Parallel velocity distribution function $F(v_z)$ at different times: $\tau=0$, 334, 525, 907. The electron distribution is modeled by a maxwellian in the perpendicular direction and by a thermal bulk and a suprathermal tail in the parallel direction (see (b) for $\tau=0$). The main normalized parameters are the following: $p=0.113$, $\boldsymbol{k}=(k_x,k_y,k_z)=(0.2,0.15,0.12)$, $\boldsymbol{k}_1=(-0.2,-0.2,-0.04)$, $\boldsymbol{k}_2=(0.4,0.35,0.16)$, $\omega_{\boldsymbol{k}}/\omega_c=0.411$, $\omega_{\boldsymbol{k}_1}/\omega_c=0.133$, $\omega_{\boldsymbol{k}_2}/\omega_c=0.273$, $\Delta\omega/\omega_c\simeq0.005$ (frequency mismatch), $v_R(m=0)=3.42$, $v_{R1}(m=0)=-3.32$, $v_{R2}(m=0)=1.7$ (Landau $m=0$ normalized resonant velocities for each of the three waves), $v_R(m=-1)=11.7$, $v_{R1}(m=-1)=-28.3$, $v_{R2}(m=-1)=7.9$ (anomalous cyclotron $m=-1$ resonant velocities), $v_R(m=1)=-4.9$, $v_{R1}(m=(1)=21.7$ , $v_{R2}(m=1)=-4.5$ (normal cyclotron $m=1$ resonant velocities), $N=50\,000$.

the total energy and impulse was sufficiently high, as their variations did not exceed 1%.

The first example we present concerns the interaction of three waves with a particle distribution presenting a suprathermal tail along the parallel direction $v_z>0$; the normalized parallel velocity $v_z$ extends up to $v_{z\max}\simeq 14$ (that is, up to several thermal velocities), whereas there are no particles with $v_z\lesssim-5$; the parallel and perpendicular velocity distribution functions of the thermal electrons are maxwellian. The three waves satisfy to the matching conditions $\boldsymbol{k}=\boldsymbol{k}_1+\boldsymbol{k}_2$ and $\omega_{\boldsymbol{k}}=\omega_{\boldsymbol{k}_1}+\omega_{\boldsymbol{k}_2}$; however, as a first step, we neglect the nonlinear wave-wave interaction term in Eq. (17). The first wave $(\omega_{\boldsymbol{k}},\boldsymbol{k})$ (resp., the third wave $(\omega_{\boldsymbol{k}_2},\boldsymbol{k}_2)$) can interact with the particles at the anomalous cyclotron resonance velocity $v_R=11.7$ (resp., $v_{R2}=7.9$) and at the Landau resonance velocity $v_R=3.42$ (resp., $v_{R2}=1.7$), whereas the second wave does not verify any resonance conditions with the particles of the distribution. Moreover, no interaction can take place at the normal cyclotron resonances as all the corresponding resonant velocities are out of the domain of the parallel particles' velocities $(-5\lesssim v_z\lesssim14)$. Figure 1a shows the evolution with the normalized time $\tau=\omega_c t/2\pi$ of the normalized energy density $E_{wk}$ (proportional to $\left|\varphi_{\boldsymbol{k}}^2\right|$) of each wave (the normalized frequencies of the three waves are $\omega_{\boldsymbol{k}}/\omega_c=0.411$, $\omega_{\boldsymbol{k}_1}/\omega_c=0.133$ and $\omega_{\boldsymbol{k}_2}/\omega_c=0.273$, respectively). One observes that the first wave $(\omega_{\boldsymbol{k}},\boldsymbol{k})$ is excited by the fan instability and saturates by particle trapping near $\tau\simeq100$, reaching a level which slowly grows with time (see also Volokitin and Krafft, 2004). As expected, the second wave cannot be resonantly excited and the third wave, which has initially a small negative growth rate, oscillates around some low noise level. The evolution of the parallel velocity distribution $F(v_z)$ is presented in Fig. 1b, showing the appearence of some perturbation near the anomalous cyclotron resonant velocity of the first wave ($v_R=11.7$) which persists during all the evolution. Meanwhile, the parallel (resp., perpendicular) kinetic energy of the particles, proportional to $\sum_{p=1}^{N} v_{zp}^2/N$ (resp., $\sum_{p=1}^{N} v_{\perp p}^2/N$) is decreasing (resp., increasing), with a net loss of particle kinetic energy (not shown here); this is characteristic of the fan instability where the deceleration of anomalous cyclotron resonant electrons allows wave excitation. Note that the Landau damping of the first wave at $v_R=3.42$ is not sufficient enough to suppress its excitation at $v_R=11.7$. Moreover, the third wave $(\omega_{\boldsymbol{k}_2},\boldsymbol{k}_2)$ begins to be weakly excited by the fan instability near $\tau\simeq700$, which can be seen on the distribution function $F(v_z)$ where some small peak is appearent near $v_R=7.9$ (see, for example, Fig. 1b for $\tau=907$).

The same wave-particle system has been studied when the interactions between the three waves are no longer neglected in Eq. (17). Figures 2a and b show the variations as a function of time $\tau$ of the normalized energy density of each wave, $E_{wk}$, and of the total wave energy density, $\sum_k E_{wk}$, respectively. In the presence of wave-wave coupling, the first wave, excited by the fan instability, exchanges quasi-periodically some energy with the two other waves, so that the periodic decrease of its energy density is accompanied by the excitation of the two other waves and inversely (see the

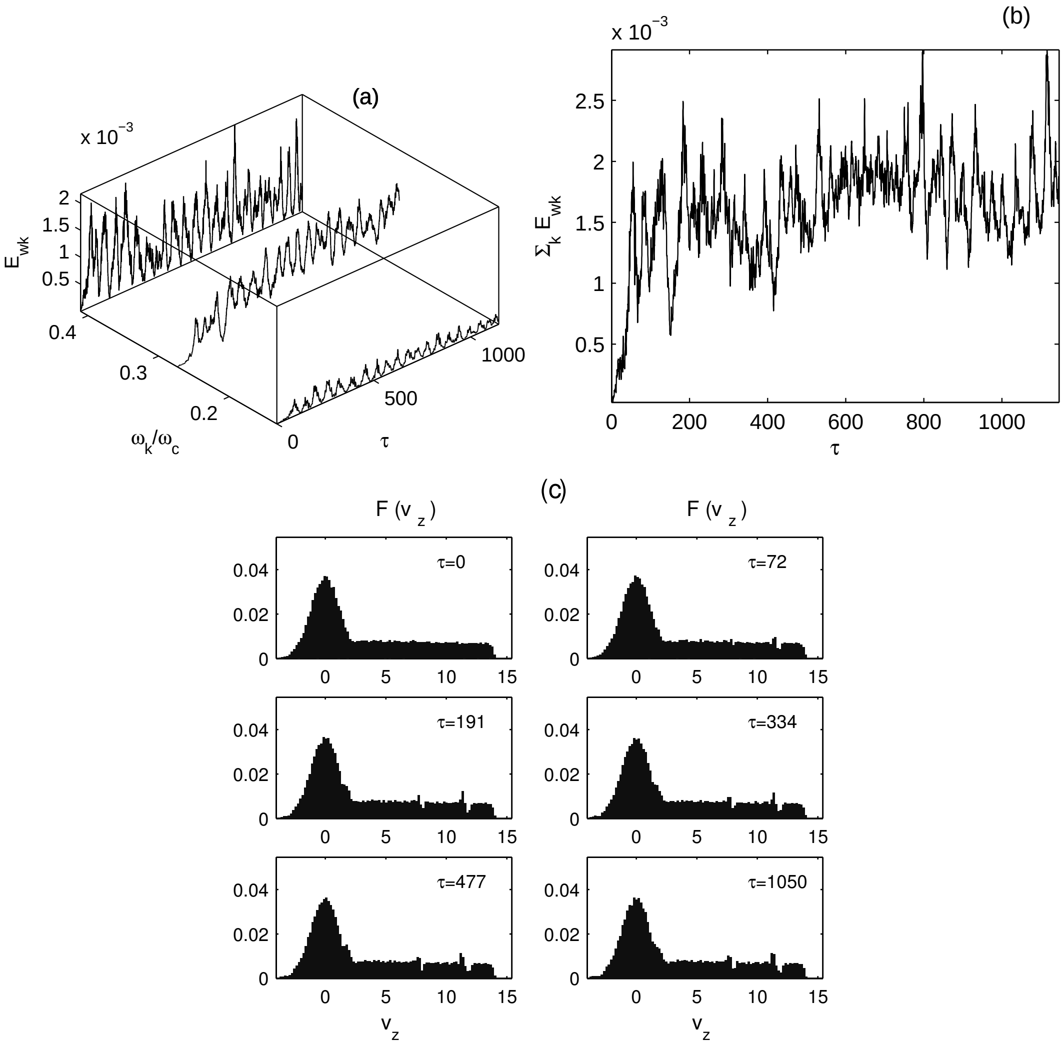


**Fig. 2.** Resonant three-waves decay ($\boldsymbol{k}$=$\boldsymbol{k}_1$+$\boldsymbol{k}_2$ and $\omega_{\boldsymbol{k}}$=$\omega_{\boldsymbol{k}_1}$+$\omega_{\boldsymbol{k}_2}$) in the presence of a suprathermal tail of electrons extending in the parallel direction $v_z>0$ (wave-wave interaction terms are not neglected). Variation as a function of the normalized time $\tau$ **(a)** of the normalized wave energy density $E_{wk}$ of each of the three waves (each wave is indicated by its normalized frequency $\omega_{\boldsymbol{k}}/\omega_c$) and **(b)** of the total normalized wave energy density $\sum_k E_{wk}$; **(c)** Parallel velocity distribution function $F(v_z)$ at different times: $\tau$=0, 72, 191, 334, 477, 1050. The main normalized parameters and the initial particle distribution functions are the same as in the Fig. 1.

Fig. 2a): the total wave energy is shared between the three waves according to the interaction coefficients (18). Moreover, the saturation stage of the total wave energy density, characterized by oscillations around a roughly constant level, now involves additional physical processes: the slow growth of the saturation level observed previously (see Fig. 1a), which could be connected with stochastic processes of wave-particle interactions where the wave eventually gains some energy, is strongly reduced when the wave energy is transfered to other waves (note that the motion of the particles in a wave field with oscillating amplitude has a complex and sometimes chaotic behavior; indeed, the examination of the trajectories of many test particles shows that stochastic processes of particle trapping and detrapping takes place, which occur for electrons located near the separatrix of the resonance region, see also Volokitin and Krafft, 2004). As shown by the Fig. 2c, where the evolution with the time of the parallel velocity distribution function $F(v_z)$ is presented, the linear stage of the interaction is dominated (see Fig. 2c for $\tau$=0, 72) by the excitation of the first wave by the fan instability at the anomalous cyclotron resonance velocity $v_R$=11.7, which overcomes the Landau damping occuring at $v_R$=3.42. Near $\tau\simeq$100, the energy gained by the first wave owing to the deceleration of the resonant particles at $v_R$=11.7 begins to be shared with the second and the third waves which are, in turn, excited. Figure 2c for $\tau$=191 shows the appearance in the parallel distribution function $F(v_z)$ of a perturbation at the anomalous resonance velocity $v_R$=7.9 (that is, the third wave is excited by the fan instability), together with a noticeable modification of $F(v_z)$ near

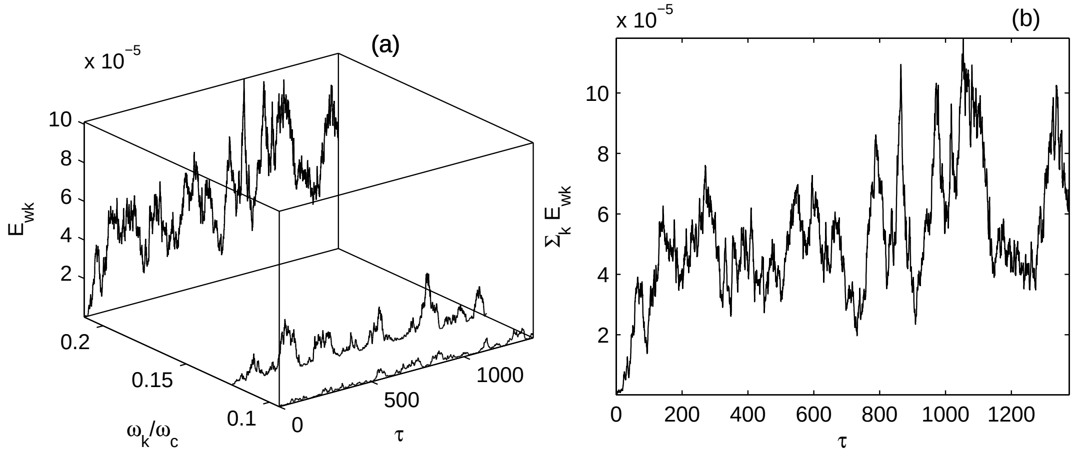


**Fig. 3.** Interaction of three waves with a particle distribution in the presence of a suprathermal tail of electrons extending in the parallel direction $v_z>0$. The waves' frequencies and wave vectors are satisfying to the matching conditions of the three-waves resonant decay: $\boldsymbol{k}=\boldsymbol{k}_1+\boldsymbol{k}_2$ and $\omega_{\boldsymbol{k}}=\omega_{\boldsymbol{k}_1}+\omega_{\boldsymbol{k}_2}$; the coupling between the three waves is neglected. **(a)** Variation as a function of the normalized time $\tau$ of the normalized wave energy density $E_{wk}$ (proportional to $\left|\varphi_{\boldsymbol{k}}^2\right|$) of each of the three waves (each wave is indicated by its normalized frequency $\omega_{\boldsymbol{k}}/\omega_c$) and **(b)** of the total normalized energy density $\sum_k E_{wk}$. The electron distribution is modeled by a maxwellian in the perpendicular direction and by a thermal bulk and a suprathermal tail in the parallel direction. The main normalized parameters are the following: $p$=0.0625, $\boldsymbol{k}=(k_x, k_y, k_z)=(0.556, -0.111, 0.125)$, $\boldsymbol{k}_1=(0.222, 0.444, 0.0625)$, $\boldsymbol{k}_2=(0.333, -0.556, 0.0625)$, $\omega_{\boldsymbol{k}}/\omega_c$=0.211, $\omega_{\boldsymbol{k}_1}/\omega_c$=0.122, $\omega_{\boldsymbol{k}_2}/\omega_c$=0.0942, $\Delta\omega/\omega_c\simeq$0.005 (frequency mismatch), $v_R(m=0)$=1.7, $v_{R1}(m=0)$=1.9, $v_{R2}(m=0)$=1.5 (Landau $m$=0 normalized resonant velocities for each of the three waves), $v_R(m=-1)$=9.7, $v_{R1}(m=-1)$=17.9, $v_{R2}(m=-1)$=17.5 (anomalous cyclotron $m=-1$ resonant velocities), $v_R(m=1)=-6.3$, $v_{R1}(m=1)=-14$, $v_{R2}(m=1)=-14.5$ (normal cyclotron $m$=1 resonant velocities), $N$=100 000.

the Landau resonance velocity $v_R$=1.7 (resonant electrons are accelerated by the third wave), indicating that significant Landau damping occurs (this effect was much weaker for the previous case when the wave-wave interactions were neglected, see Fig. 1b). Thus, the presence of wave coupling effects enhance the interaction of the waves with the particles, as shown by the progressive and significant modification of the electron distribution function $F(v_z)$ during the time evolution (see Fig. 2c for $\tau>191$), for example, one can see near $v_R$=1.7 the formation of a plateau (see Fig. 2c for $\tau\simeq191$) followed by the appearance of a small peak (see the Fig. 2c for $\tau$=477) which can, in turn, allow the excitation of the third wave by the bump-in-tail instability owing to the presence of a positive slope (indeed, one observes an increase in the saturation level of this wave for $\tau\gtrsim400$, see Fig. 2a).

Let us now consider three waves satisfying the matching conditions $\boldsymbol{k}=\boldsymbol{k}_1+\boldsymbol{k}_2$ and $\omega_{\boldsymbol{k}}=\omega_{\boldsymbol{k}_1}+\omega_{\boldsymbol{k}_2}$, with the first wave $(\omega_{\boldsymbol{k}}, \boldsymbol{k})$ interacting with the particles at two resonance velocities, $v_R$=1.7 (Landau) and $v_R$=9.7 (anomalous cyclotron). The second and the third waves are resonant with the bulk particles at the Landau resonance velocities $v_R$=1.9 and $v_R$=1.5, respectively. Initially, the first wave is unstable and the two others are damped. Numerical simulations performed without including the wave-wave interaction terms in Eq. (17) show that the first wave with $\omega_k/\omega_c$=0.211 is excited by the fan instability (see Fig. 3a), whereas the third wave's amplitude ($\omega_{\boldsymbol{k}_2}/\omega_c$=0.0942) remains very small during the entire time evolution (compare Figs. 3a and 3b), the second wave ($\omega_{\boldsymbol{k}_1}/\omega_c$=0.122) is weakly excited by the bump-in-tail instability driven by the small modification of the parallel velocity distribution function in the region where this wave can interact at the Landau resonance with the particles. Without this modification, only Landau damping occurs and the second wave could not be excited at all through resonant wave-particle interactions.

When the wave coupling effects are included in the numerical calculations (see the Fig. 4b), the maximum and the saturation level of the total wave energy density remain roughly the same, as in the previous case, but the redistribution of the energy between the waves during the evolution time is quite different. The first wave shares its energy with the two others through nonlinear coupling (one can see in the Fig. 4a several clear oscillations with a period of the order of $\Delta\tau\simeq20$), which leads to a strong modification of the parallel velocity distribution in the region where the two daughter waves are resonant with the particles (that is, within the domain $1.5\lesssim v_R\lesssim1.9$): as a result, lower energy particles are accelerated (not shown here). Meanwhile, the variations of the parallel and the perpendicular kinetic energies between the initial and the final evolution times, that is, $\Delta\left(\sum_{p=1}^N v_{zp}^2/N\right)$ and $\Delta\left(\sum_{p=1}^N v_{\perp p}^2/N\right)$, are 4 times larger than when the wave-wave interactions are neglected, whereas the net loss of kinetic energy is roughly the same.

The nonlinear evolution of a set of three lower hybrid waves interacting with suprathermal electrons at various

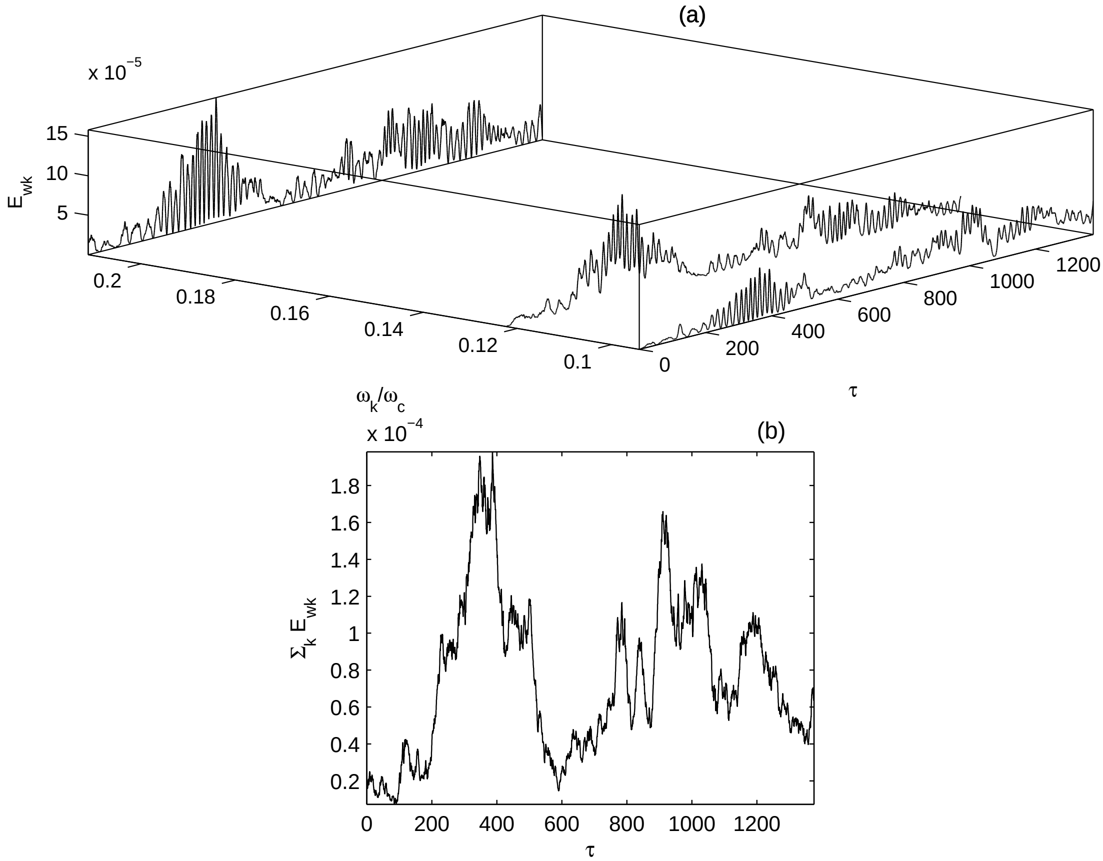


**Fig. 4.** Resonant three-waves decay ($\boldsymbol{k}=\boldsymbol{k}_1+\boldsymbol{k}_2$ and $\omega_{\boldsymbol{k}}=\omega_{\boldsymbol{k}_1}+\omega_{\boldsymbol{k}_2}$) in the presence of a suprathermal tail of electrons extending in the parallel direction $v_z>0$ (wave-wave interaction terms are not neglected). Variation as a function of the normalized time $\tau$ of **(a)** the normalized wave energy density $E_{wk}$ of each of the three waves (each wave is indicated by its normalized frequency $\omega_{\boldsymbol{k}}/\omega_c$) and **(b)** the total normalized wave energy density $\sum_k E_{wk}$. The main normalized parameters and the initial particle distribution functions are the same as in Fig. 3.

resonance velocities shows that a competition between excitation (due to the fan instability with tail electrons or to the bump-in-tail instability at the Landau resonances) and damping processes (involving bulk electrons at the Landau resonances) takes place for each wave, depending on the strength of the wave-wave coupling, on the linear growth rates of the waves and on the modifications of the particles' distributions resulting from the linear and nonlinear wave-particle interactions. Moreover, it is shown that the energy carried by the suprathermal electron tail is more effectively transfered to lower energy electrons in the presence of wave-wave interactions.

*Acknowledgements.* The authors acknowledge the Centre National de la Recherche Scientifique (CNRS, PICS 1310, France), the Institut Universitaire de France (Paris), the Russian Academy of Sciences and the Russian Foundation for Basic Research (RFBR, Grant No. 01-05–22003 NCNIa) for their financial support.

Topical Editor T. Pulkkinen thanks B. Vasquez and another referee for their help in evaluating this paper.

## References

Ergun, R. E., Delory, G. T., Klementis, E., Carlson, C. W., McFadden, J. P., and Roth, I.: VLF waves growths from dispersive bursts of field-aligned electron fluxes, J. Geophys. Res., 98, A3, 3777–3787, 1993.

Ergun, R. E., Larson, D., Lin, R. P., McFadden, J. P., Carlson, C. W., Anderson, K. A., Muschietti, I., McCarthy, M., Parks, G. K., Rème, H., Bosqued, J. M., D'Uston, C., Sanderson, T. R., Wenzel, K. P., Kaiser, M., Lepping, R. P. Bale, S. D., Kellogg, P., and Bougeret, J. L.: Wind spacecraft observations of solar impulsive electron events associated with solar type III radio bursts, Astrophys. J., 503, 435–445, 1998.

Haber, I., Huba, J. D., Palmadesso, P., and Papadopoulos, K.: Slope reversal of a monotonically decreasing electron tail in a strong magnetic field, Phys. Fluids, 21, 6, 1013–1016, 1978.

Hoppe, M. M., Russell, C. T., Eastman, T. E., and Frank, L. A.: Characteristics of the ULF waves associated with upstream ion beams, J. Geophys. Res., 87, A2, 643–650, 1982.

Kadomtsev, B. B. and Pogutse, O. P.: Electric conductivity of a plasma in a strong magnetic field, Soviet Phys. JETP, 26, 1146, 1967.

Kellogg, P. J., Goetz, K., Howard, R. L., and Monson, S. J.: Evidence for Langmuir wave collapse in the interplanetary plasma,

Geophys. Res. Lett., 19, 1303, 1992a.
Kellogg, P. J., Goetz, K., Lin, N., Monson, S. J., Balogh, A., Forsyth, R. J., and Stone, R. G.: Low-frequency magnetic signals associated with Langmuir waves, Geophys. Res. Lett., 19, 12, 1299–1302, 1992b.
Kovalenko, V. P.: Electron bunches in nonlinear collective beam-plasma interaction, Sov. Phys. Usp., 26, 116, 1983.
Krafft, C., Volokitin, A., and Flé, M.: Nonlinear electron beam interaction with a wave packet, Phys. Plasmas, 7, 4423–4432, 2000.
Krafft, C. and Volokitin, A.: Resonant electron beam interaction with several lower hybrid waves, Phys. Plasmas, 9, 2786–2797, 2002.
Krafft, C. and Volokitin, A.: Interaction of a wave packet with a thin electron beam spiraling in a magnetized plasma, Phys. Plasmas, 10(8), 3093–3102, 2003a.
Krafft, C. and Volokitin, A.: Interaction of suprathermal solar wind electron fluxes with sheared whistler waves: Fan instability, Ann. Geophys., 21, 1393–1403, 2003b.
Lin, R. P., Potter, D. W., Gurnett, D. A., and Scarf, F. L.: Energetic electrons and plasma waves associated with a solar type III radio burst, Astrophys. J., 251, 364–373, 1981.
Lin, R. P., Levedahl, W. K., Lotko, W., Gurnett, D. A., and Scarf, F. L.: Evidence for nonlinear wave-wave interaction in solar type III radio bursts, Astrophys. J., 308, 954–965, 1986.
Lin, N., Kellogg, P. J., MacDowall, R. J., Scime, E. E., Balogh, A., Forsyth, R. J., McComas, D. J., and Phillips, J. L.: Very low frequency waves in the heliosphere: Ulysses observations, J. Geophys. Res., 103, A6, 12 023–12 035, 1998.
Matsiborko, N. G., Onischenko, I. N., Shapiro, V. D., and Shevchenko, V. I.: On nonlinear theory of instability of a monoenergetic electron beam in plasmas, Plasma Phys., 14, 591–600, 1972.
Matsiborko, N. G., Onischenko, I. N., Fainberg, Ya. B., and Shapiro, V. D.: Appearence of turbulence during the interaction of a monoenergetic beam with a plasma, Sov. Phys. JETP, 36, 460–465, 1973.
Mikhailovskii, A. B.: Theory of Plasma Instabilities, Consultants Bureau, New York, 1974.
Moullard, O., Burgess, D., and Bale, S. D.: Whistler waves observed during an in-situ solar type III radio bursts, Astron. Astrophys., 335, 703–708, 1998.
Moullard, O., Burgess, D., Salem, C., Mangeney, A., Larson, D. E., Bale, S. D.: Whistler waves, Langmuir waves and single loss cone electron distribution inside a magnetic cloud: Observations, J. Geophys. Res., 106, A5, 8301–8313, 2001.
Muschietti, L., Roth, I., and Delory, G.: Oblique turbulence driven by field-aligned electron fluxes in the auroral ionosphere, J. Geophys. Res., 102, A12, 27 217–27 226, 1997.
O'Neil, T. M., Winfrey, J. H., and Malmberg, J. H.: Nonlinear interaction of a small cold beam and a plasma, Phys. Fluids, 14, 1204–1212, 1971.
Omelchenko, Yu. A., Shapiro, V. D., Shevchenko, V. I., Ashour-Abdalla, M., and Schriver, D.: Modified lower hybrid fan instability excited by precipitating auroral electrons, J. Geophys. Res., 99, A4, 5965–5975, 1994.
Pivovarov, V., Burke, A., Ride, S. K., and Shapiro, V. D.: Excitation of VLF waves by an electron beam injected into the ionosphere, J. Geophys. Res., 100, 17 515–17 526, 1995.
Shapiro, V. D. and Shevchenko, V. I.: Quasi-linear theory of relaxation of an electron beam in a magnetoactive plasma, Soviet Phys. JETP, 27, 635–642, 1968.
Shapiro, V. D. and Shevchenko, V. I.: Contribution to the nonlinear theory of relaxation of a monoenergetic beam in a plasma, Soviet Phys. JETP, 33, 555–561, 1971.
Reiner, M. J., Fainberg, J., and Stone, R. G.: Detection of fundamental and harmonic type III radio emission and the associated Langmuir waves at the source region, Astrophys. J., 394, 340, 1992.
Stone, R. G., MacDowall, R. J., Fainberg, J., Hoang, S., Kaiser, M. L., Kellogg, P. J., Lin, N., Osherovich, V. A., Bougeret, J. L., Canu, P., Cornilleau-Wehrlin, N., Desch, M. D., Goetz, K., Goldstein, M. L., Harvey, C. C., Lengyel-Frey, D., Manning, R., Reiner, M. J., Steinberg, J. L., and Thejappa, G.: Ulysses radio and plasma wave observations at high southern heliograthic latitudes, Science, 268, 1026–1029, 1995.
Thejappa, G., Wentzel, D. G., and Stone, R. G.: Low-frequency waves associated with Langmuir waves in solar wind, J. Geophys. Res., 100, A3, 3417–3426, 1995.
Thejappa, G. and MacDowall, R. J.: Evidence for strong and weak turbulence processes in the source region of a local type III radio burst, Astrophys. J., 498, 465–478, 1998.
Volokitin, A. and Krafft, C.: Dynamically stable electron bunches in beam interaction with an electromagnetic wave packet, JETP Lett., 71, 262–267, 2000.
Volokitin, A. and Krafft, C.: Electron beam interaction with lower hybrid waves at cyclotron and Cherenkov resonances, Phys. Plasmas, 8, 3748–3758, 2001a.
Volokitin, A. and Krafft, C.: Spiral electron beam interaction with whistler waves at cyclotron resonances, Phys. Plasmas, 8, 4960–4971, 2001b.
Volokitin, A. and Krafft, C.: Interaction of suprathermal electron fluxes with lower hybrid waves, Phys. Plasmas, in press, 2004.
Zhang, Y. L., Matsumoto, H., Kojima, H., and Omura, Y.: Extremely intense whistler mode waves near the bow shock: Geotail observations, J. Geophys. Res., 104, A1, 449–461, 1999.